

## Research Article

# Appraisal on Textured Grain Growth and Photoconductivity of ZnO Thin Film SILAR

Deepu Thomas,<sup>1,2</sup> Sunil C. Vattappalam,<sup>2</sup> Sunny Mathew,<sup>2</sup> and Simon Augustine<sup>2</sup>

<sup>1</sup> Research and Development Centre, Bharathiar University, Coimbatore 641046, India

<sup>2</sup> Department of Physics, St. Thomas College, Pala, Kottayam 686574, India

Correspondence should be addressed to Deepu Thomas; [deepuskariankal@gmail.com](mailto:deepuskariankal@gmail.com)

Received 26 April 2014; Revised 24 June 2014; Accepted 3 July 2014; Published 13 July 2014

Academic Editor: Salah S. Massoud

Copyright © 2014 Deepu Thomas et al. This is an open access article distributed under the Creative Commons Attribution License, which permits unrestricted use, distribution, and reproduction in any medium, provided the original work is properly cited.

ZnO thin films were prepared by successive ionic layer adsorption reaction (SILAR) method. The textured grain growth along *c*-axis in pure ZnO thin films and doped with Sn was studied. The structural analysis of the thin films was done by X-ray diffraction and surface morphology by scanning electron microscopy. Textured grain growth of the samples was measured by comparing the peak intensities. Textured grain growth and photo current in ZnO thin films were found to be enhanced by doping with Sn. ZnO thin film having good crystallinity with preferential (002) orientation is a semiconductor with photonic properties of potential benefit to biophotonics. From energy dispersive X-ray analysis, it is inferred that oxygen vacancy creation is responsible for the enhanced textured grain growth in ZnO thin films.

## 1. Introduction

The synthesis and characterization of ZnO thin film have been an active area of research for nearly half a century. ZnO with wurtzite structure [1] is an n-type semiconductor with direct band gap of 3.37 eV [2, 3] and high electronic mobility. Due to wide and direct band gap semiconductor, nanostructure ZnO thin films have attracted more attention in optoelectronic devices [4]. The transparent conductive oxide (TCO) electrodes using Al-doped ZnO have been used as powerful candidate materials for ITO transparent electrodes. ZnO thin films have attracted much attention because they can be tailored to possess high electrical conductivity, high infrared reflectance, and high visible transmittance upon applying different techniques [5–8]. Different methods have been applied to obtain ZnO thin films. The important techniques include magnetron sputtering [6], chemical bath deposition [9], sol-gel [10], and spray pyrolysis [11]. Chemical deposition techniques are relatively low cost processes and can be easily scaled up for industrial application. Among the thin film deposition methods, double dip technique from aqueous solutions is the simplest and the most economical one. Double dip method otherwise called SILAR method

(successive immersion layer adsorption reaction) [5, 12, 13] also offers the opportunity of doping the host ions with impurities on different kinds, shapes, and sizes on substrates with ease. Zinc oxide crystallites with preferential grain growth along *c*-axis are desirable for applications such as UV diode lasers, piezoelectric surface acoustic wave or acoustic-optic devices, and gas sensors [4]. There are reports that textured grain growth along *c*-axis in ZnO thin films is enhanced by doping and annealing. Controllable n-type doping is easily achieved by substituting Zn with group IV elements such as Sn [5, 6]. Moreover, the band gap of the material can be tuned from 3.37 to 3.11 eV if it is doped with group IV metal ions.

In course of the present investigations, textured grain growth in Sn-doped ZnO thin films and photoconductivity were studied. A possible mechanism for the textured grain growth is also investigated. Such studies are not yet reported.

## 2. Experimental

ZnO thin films were prepared by successive ionic layer adsorption reaction (SILAR) method, in which the ZnO thin film was coated on the glass substrate (26 \* 76 mm) by

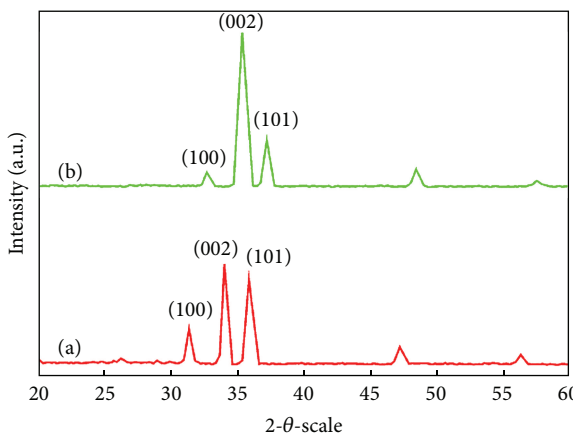


FIGURE 1: (a) and (b) show the XRD pattern of pure and doped sample.

alternately dipping the substrate in sodium zincate bath at room temperature and then in hot water maintained at 90–95°C. Sankapal et al. [14] had already used this method for preparing Cu<sub>2</sub>O thin films. Sodium zincate bath was prepared by using 1 M zinc sulphate [ZnSO<sub>4</sub>·7H<sub>2</sub>O] and 2 M sodium hydroxide [NaOH]. Tin doping was done by adding stannous chloride (tin chloride) in sodium zincate bath. The doping concentration of tin was 5 atm%. Before deposition, the glass substrates were cleaned by chromic acid followed by cleaning with acetone. The well-cleaned substrates were immersed in the chemical bath for 10 sec followed by immersion in hot water for the same time and this was repeated for 100 times. These samples were annealed at 450°C for half an hour in air. The structural analysis of the thin films was done by X-ray diffraction (XRD) and surface morphology by scanning electron microscopy (SEM). X-ray diffraction was performed on Bruker AXS-8 using CuK<sub>α</sub> radiation and SEM micrographs were taken by using JEOL-JSM6490. Chemical elemental stoichiometry was examined from energy-dispersive X-ray analysis (EDAX) linked with SEM unit. The resistance of ZnO thin film at room temperature was measured by Keithley 2100 6 1/2 Digital Multimeter. The optical absorbance was measured in the wavelength range of 190–1100 nm by means of a UV-VIS spectrophotometer. The photoconductivity of the samples was studied by Keithley 6485 picometer. Textured grain growth of the samples was measured by using a texture index (T.I.), which is the ratio of the intensities of (002) reflection ( $2\theta = 34^\circ$ ) to (101) reflection ( $2\theta = 36^\circ$ ) in the XRD:

$$\text{T.I.} = \frac{I_{002}}{I_{101}}. \quad (1)$$

### 3. Results and Discussion

**3.1. Structural and Morphological Characterization.** XRD patterns of ZnO thin films of pure and doped samples are depicted in Figures 1(a) and 1(b). It is seen from the figures that the (002) peak appears with maximum intensity at  $2\theta = 34^\circ$ . The other peaks at  $31^\circ$  and  $36^\circ$  can be associated with (100), (101) reflections of ZnO, as expected

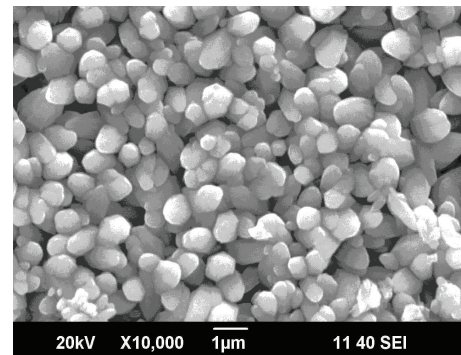


FIGURE 2: SEM micrograph of pure ZnO thin film.

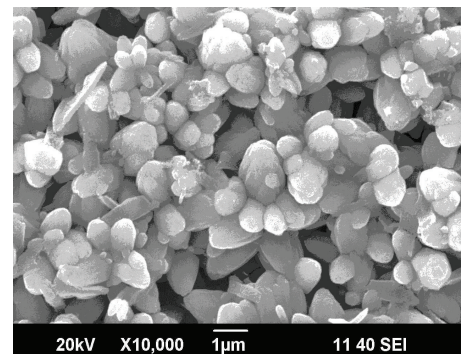


FIGURE 3: SEM micrograph of Sn-doped ZnO thin film.

for wurtzite hexagonal ZnO structure (JCPDS number 36-1-1451). In particular, it is clearly observed that the intensity of the (002) peak was enhanced by doping with Sn. The (002) diffraction peak exhibited a higher intensity, showing the fact that the textured grain growth is along (002) direction. Table 1 gives the textured grain growth, resistance, and band gap of pure and doped samples. Figures 2 and 3 show the SEM micrographs of the pure sample and doped sample. From Figures 1(a) and 1(b) and Table 1, it is clear that there is significant textured grain growth in tin-doped sample. The needle-like as well as flowered structure of ZnO is evident in the SEM micrograph of the pure sample (Figure 2). But when sample was doped with Sn, the needle-like structure disappeared and flowered structure became more prominent (Figure 3). The average grain size of the ZnO crystals in the films was calculated by using Scherrer's formula:  $D = 0.9\lambda/\beta \cos \theta$ , where  $D$  is the grain size,  $\lambda$  is the wavelength of X-ray used,  $\beta$  is the FWHM (full width half maximum), and  $\theta$  is Bragg diffraction angle of the XRD peak. From the studies, the grain size of the Sn-doped sample was found to be in the range 27.35 nm (Table 1). The dislocation density  $\delta = 1/D^2$ , where  $D$  is the grain size. Dislocation density gives the degree of crystallinity. Therefore, larger values of  $D$  indicate better crystallization of the films. Thus the increase in texture index indicates increase in crystallinity in Sn-doped ZnO thin film. ZnO thin films having good crystallinity with preferential (002) orientation is a prerequisite for the

TABLE 1: Texture index, grain size, resistance, and band gap of pure and doped samples.

Sample number	Sample details	Orientation index (O.I.)	Grain size ( $D$ ) in nm	Resistance in K $\Omega$ at room temp.	Band gap in eV
1	Pure sample	1.21	18	9	3.3
2	Sn-doped	4.61	27.35	2.25	3.11

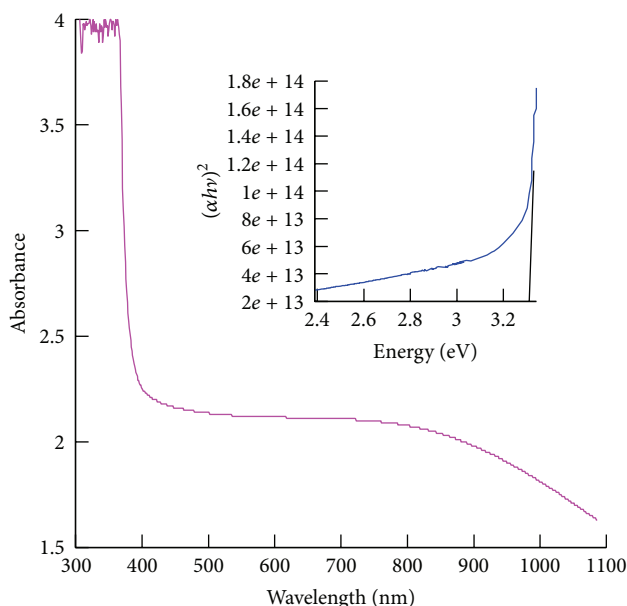


FIGURE 4: Absorbance for the sample pure ZnO thin film. The inset indicates optical band gap energy of the sample.

fabrication of devices like UV diode lasers, acoustic-optic devices, and gas sensors.

From Figures 1(a), 1(b), 2, and 3 and from Table 1 it is clear that textured grain growth in Sn-doped sample is increased significantly. The SEM micrographs confirm the textured grain growth in the sample.

**3.2. Resistance Measurements.** The thin film resistivity was strongly influenced by the interaction of the conduction electrons with the surface. In other words, it is a measure of the material surface that is inherently resistant to the current flow. The grain size and resistance of ZnO thin films measured at room temperature are given in Table 1. It shows that, as the grain size increases, the resistance of the film decreases; that is, resistance is inversely proportional to the grain size. One of the reasons for this process is due to the decrease in grain boundary when the grain sizes increase. Another one is due to the contribution from Sn ions on the substitutional site of Zn ions and Sn-interstitial atoms.

**3.3. Optical Properties of Nanocrystalline ZnO Films.** Figure 4 shows the optical absorbance spectrum of ZnO thin films annealed at 450°C in air for half an hour using UV-visible region from 200 nm to 800 nm. The corresponding optical band gap of ZnO thin film is estimated by extrapolation of the linear relationship between  $(\alpha h v)^2$  and  $h v$  according to

the equation  $h v = A(h v - E_g)^{1/2}$  where  $\alpha$  is the absorption coefficient,  $h v$  is the photon energy,  $E_g$  is the optical band gap, and  $A$  is a constant. Figure 4 (inset) is the plot of  $(\alpha h v)^2$  versus energy  $h v$ . The single slope in the figure suggests that the sample has direct and allowed transition. The band gap value of pure ZnO thin film is found to be 3.30 eV which is slightly smaller than that of bulk ZnO (3.37 eV). This difference is due to the factors like the granular structure, the nature and concentration of precursors, the structural defects of the films, and so forth [15]. The band gap is also calculated for the sample doped with tin and annealed in air. The corresponding values are reported in Table 1. It shows that band gap decreases with increase in the grain size of film; that is, band gap is inversely proportional to the grain size. The resistance decreases with the increase in the grain size, as the grain boundary decreases. In the case of both samples the grain size was found to be inversely proportional to band gap.

**3.4. Photoconductivity Studies.** Photoconductivity is a phenomenon in which samples become electrically conductive due to the absorption of electromagnetic radiation. When light is absorbed by samples, the number of free electrons and holes changes and raises its electrical conductivity [16]. The photo current and dark current of pure and doped sample are shown in Figures 5 and 6. From the figures it is clear that both the dark and photo current of the samples increase linearly with applied field. For the same applied field, the photo current is greater than dark current which reveals the positive photoconducting behaviour of sample. In case of the Sn-doped sample photo current and dark current are more than the pure sample. This infers that doped samples were able to generate more photo current than the pure samples. This makes them promising candidate for solar cells. The results also indicate that the ZnO is beneficial to photodynamic therapy [17].

**3.5. Elemental Analysis by EDAX.** Energy-dispersive X-ray spectroscopy (EDS or EDX) is an analytical technique used for the elemental analysis or chemical characterization of a sample. Theoretically expected stoichiometric masses% of Zn and oxygen are 80.3 and 19.7. The atomic percentages of oxygen in the pure and doped samples are 27.54 and 24.20, respectively. From the above values, it is clear that, as the texture index increases, the oxygen content of the samples decreases. This means that oxygen vacancy is more in samples that have more textured grain growth. Native or intrinsic defects are the reasons behind this vacancy creation [18]. It is reported that Sn-doping will create oxygen vacancies due to the substitution of Zn by Sn. This confirms that oxygen vacancy creation is the mechanism behind the enhanced textured grain growth.

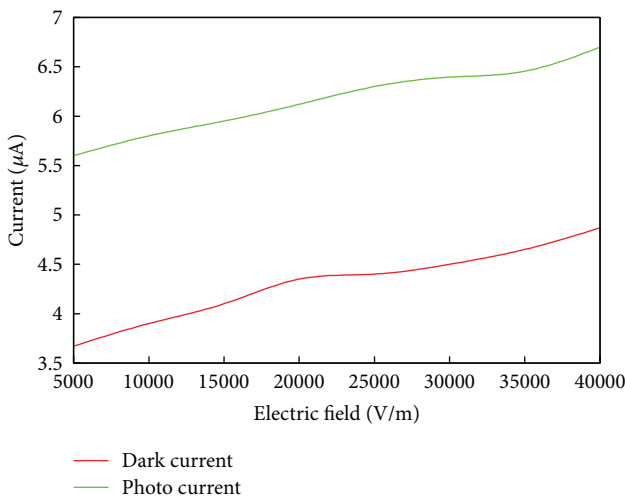


FIGURE 5: Field dependent photoconductivity of pure ZnO thin film.

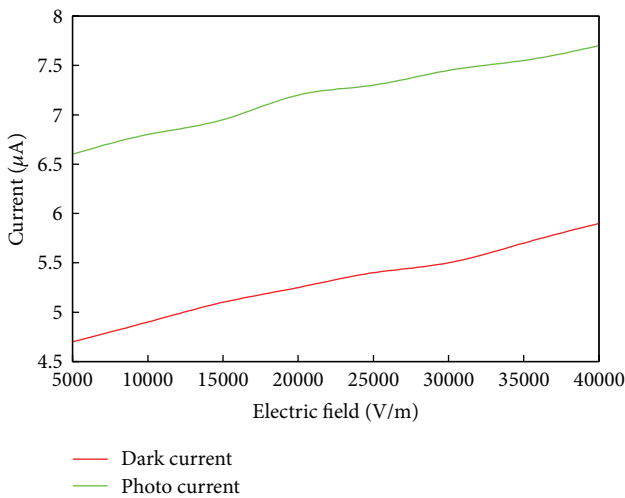


FIGURE 6: Field dependent photoconductivity of Sn-doped ZnO thin film.

## 4. Conclusion

From the studies, the following findings can be drawn. Textured grain growth in ZnO thin films enhanced significantly by Sn-doping. From the SEM micrographs it is found that as the textured grain growth increases the needle-like structure disappears and flowered structure becomes prominent. When the textured grain growth increases, crystallinity of the thin film improves, photo current increases, and resistance and band gap decrease. ZnO thin film having good crystallinity with preferential (002) orientation is a semiconductor with photonic properties of potential benefit to biophotonics. From energy-dispersive X-ray analysis, it is inferred that oxygen vacancy creation is responsible for the enhanced textured grain growth in ZnO by Sn-doping.

## Conflict of Interests

The authors declare that there is no conflict of interests regarding the publication of this paper.

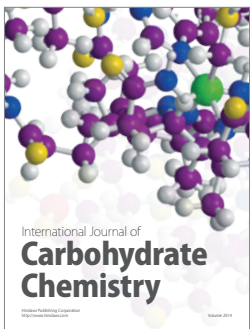
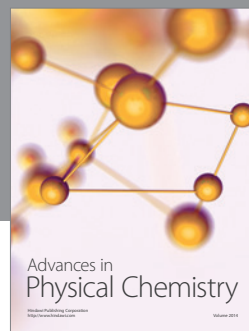
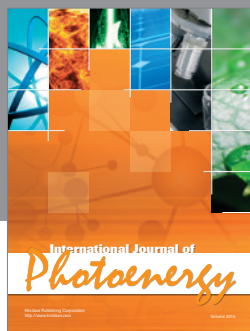
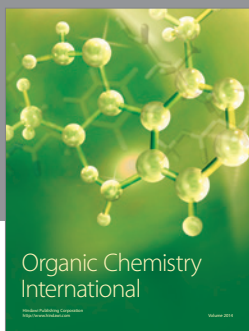
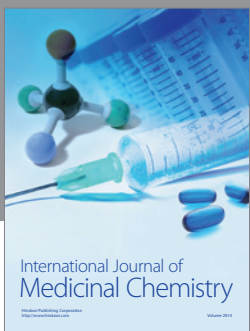
## Acknowledgment

The authors are thankful for the financial support from University Grants Commission, Government of India, through a research Grant (MRP(S)-986/10-11/KLMG027/UGC-SWRO).

## References

- [1] G. Xiangdong, L. Xiaomin, and Y. Weidong, "Preparation and characterization of highly oriented ZnO film by ultrasonic assisted SILAR method," *Journal Wuhan University of Technology, Materials Science Edition*, vol. 20, no. 3, pp. 23–26, 2005.
- [2] B. Zhou, A. V. Rogachev, Z. Liu, D. G. Piliptsov, H. Ji, and X. Jiang, "Effects of oxygen/argon ratio and annealing on structural and optical properties of ZnO thin films," *Applied Surface Science*, vol. 258, no. 15, pp. 5759–5764, 2012.
- [3] V. Shelke, B. K. Sonawane, M. P. Bhole, and D. S. Patil, "Electrical and optical properties of transparent conducting tin doped ZnO thin films," *Journal of Materials Science: Materials in Electronics*, vol. 23, no. 2, pp. 451–456, 2012.
- [4] T. Yen, D. Strome, S. J. Kim, A. N. Cartwright, and W. A. Anderson, "Annealing studies on zinc oxide thin films deposited by magnetron sputtering," *Journal of Electronic Materials*, vol. 37, no. 5, pp. 764–769, 2008.
- [5] J. H. Park, J. M. Shin, S. Cha et al., "Deposition-temperature effects on AZO thin films prepared by RF magnetron sputtering and their physical properties," *Journal of the Korean Physical Society*, vol. 49, no. 2, pp. S584–S588, 2006.
- [6] R. Chandramohan, V. Dhanasekaran, S. Ezhilvizhian et al., "Spectral properties of aluminium doped zinc oxide thin films prepared by SILAR method," *Journal of Materials Science: Materials in Electronics*, vol. 23, no. 2, pp. 390–397, 2012.
- [7] J. Son, J. Shim, and N. Cho, "Variations in electrical and physical properties of Al:ZnO films with preparation conditions," *Metals and Materials International*, vol. 17, no. 1, pp. 99–104, 2011.
- [8] P. P. Murmu, J. Kennedy, B. J. Ruck et al., "Effect of annealing on the structural, electrical and magnetic properties of Gd-implanted ZnO thin films," *Journal of Materials Science*, vol. 47, no. 3, pp. 1119–1126, 2012.
- [9] H. Zhu, J. Hüpkens, E. Bunte, A. Gerber, and S. M. Huang, "Influence of working pressure on ZnO:Al films from tube targets for silicon thin film solar cells," *Thin Solid Films*, vol. 518, no. 17, pp. 4997–5002, 2010.
- [10] W. Luo, T. Tsai, J. Yang, W. Hsieh, C. Hsu, and J. Fang, "Enhancement in conductivity and transmittance of zinc oxide prepared by chemical bath deposition," *Journal of Electronic Materials*, vol. 38, no. 11, pp. 2264–2269, 2009.
- [11] Y. Kokubun, H. Kimura, and S. Nakagomi, "Preparation of ZnO thin films on sapphire substrates by sol-gel method," *Japanese Journal of Applied Physics*, vol. 42, part 2, no. 8A, p. 904, 2003.
- [12] Y. Lee, H. Kim, and Y. Roh, "Deposition of ZnO thin films by the ultrasonic spray pyrolysis technique," *Japanese Journal of Applied Physics*, vol. 40, no. 4, part 1, pp. 2423–2428, 2001.
- [13] H. M. Pathan and C. D. Lokhande, "Deposition of metal chalcogenide thin films by successive ionic layer adsorption and

- reaction (SILAR) method," *Bulletin of Materials Science*, vol. 27, no. 2, pp. 85–111, 2004.
- [14] B. R. Sankapal, R. S. Mane, and C. D. Lokhande, "Preparation and characterization of Sb<sub>2</sub>S<sub>3</sub> thin films using a successive ionic layer adsorption and reaction (SILAR) method," *Journal of Materials Science Letters*, vol. 18, no. 18, pp. 1453–1455, 1999.
- [15] M. Saleem, L. Fang, A. Wakeel, M. Rashad, and C. Y. Kong, "Simple preparation and characterization of nano-crystalline Zinc Oxide thin films by sol-gel method on glass substrate," *World Journal of Condensed Matter Physics*, vol. 2, no. 6, pp. 10–15, 2012.
- [16] M. H. Huang, S. Mao, H. Feick et al., "Room-temperature ultraviolet nanowire nanolasers," *Science*, vol. 292, no. 5523, pp. 1897–1899, 2001.
- [17] S. John, S. Marpu, J. Li et al., "Hybrid zinc oxide nanoparticles for biophotonics," *Journal of Nanoscience and Nanotechnology*, vol. 10, no. 3, pp. 1707–1712, 2010.
- [18] A. Janotti and C. G. Van de Walle, "Fundamentals of zinc oxide as a semiconductor," *Reports on Progress in Physics*, vol. 72, no. 12, Article ID 126501, 2009.



Hindawi

Submit your manuscripts at  
<http://www.hindawi.com>

